

Problem of plane strain state of two-layer body in dynamic elastic-plastic formulation (Part I)

Vladislav Bogdanov

Progressive Research Solutions Pty. Ltd.
Buller Rd 28/2, Artarmon, Sydney, Australia 2064
vladislav_bogdanov@hotmail.com, orcid.org/0000-0002-3424-1801

Received 01.08.2022, accepted 06.09.2022
<https://doi.org/10.32347/uwt.2022.12.1101>

Abstract. The design of composite and reinforced or armed materials is a requirement of the modern level of production and life. Many methods of calculation and design of such materials are successfully used. In this article, for the design of composite and reinforced materials, a technique for solving dynamic contact problems in more precise an elastic-plastic mathematical formulation is used. To consider the physical nonlinearity of the deformation process, the method of successive approximations is used, which makes it possible to reduce the nonlinear problem to a solution of the sequences of linear problems. In contrast to the traditional plane strain, when one normal stress is equal to a certain constant value, for a more accurate description of the deformation of the sample, taking into account the possible increase in longitudinal elongation, we present this normal stress as a function that depends on the parameters that describe the bending of a prismatic body that is in a plain strain state. The problem of a plane strain state of a beam made from the composite reinforced double-glazed material is being solved. The reinforced or armed material consists of two layers: the upper (first) thin layer of solid steel and the lower (second) main layer of glass. Glass is a non-crystalline, often transparent amorphous solid, that has widespread practical and technological use in the modern industry. The most familiar types of manufactured glass are "silicate glasses" based on the chemical compound silica (silicon dioxide, or quartz). Glass has high strength and is not affected by the processes of aging of the material, corrosion, and creep. In addition, this material is cheap and widely available. Glass



Vladislav Bogdanov
Director of Progressive Research Solutions
PhD (mathematics and physics)
Snr. Res. Ass.

can be strengthened, for example, in a melt quenching process. If the cooling is fast enough (relative to the characteristic crystallization time), then crystallization is prevented, and instead the disordered atomic configuration of the supercooled liquid is frozen into a solid state. This increases the strength properties of the glass. The reinforced composite beam is rigidly linked to an absolutely solid base and on which an absolutely solid impactor acts from above in the centre on a small area of initial contact.

Keywords: Plane, strain, impact, composite material, armed material, reinforced material, elastic-plastic, deformation.

INTRODUCTION

Glass is a very strong and very fragile material at the same time. The fragility of glass is due to the fact that there are many microcracks on the surface, and when a load is applied to the glass surface, these microcracks begin to grow and lead to the destruction of glass products. If we glue or immobilize the tops of microcracks on the surface, we will get a strong reinforced armed material that will be lighter, stronger and

not subject to degradation of material properties such as aging, corrosion and creep. The upper reinforcing layer of metal or steel can be applied to the glass surface so that metal or steel atoms penetrate deeply, fill microcracks and bind their tops. The top layer can be quite thin. The adhesion between the layers is considered perfectly rigid. The issue of practical provision of such coupling is an important component of technological implementation. In the E.O. Paton Institute of Electric Welding of the National Academy of Sciences of Ukraine in the early 2000s, the technology of welding ceramic parts was developed. A copper membrane was clamped between two ceramic parts. A powerful electric impulse was applied to the membrane, as a result of which the copper membrane instantly evaporated and the copper atoms penetrated deep into the structural pores, capillaries and microcracks of the material. Due to this, the welding of ceramic parts was carried out with sufficient strength. In our case, layers of glass and steel can be rigidly connected using this technology. Steel is a polycrystalline material with many microcracks between the grains among the carbides. Therefore, atoms of copper, or other material according to the technology, penetrate into the microcracks of glass and steel and immobilize the tops of the microcracks of the materials.

Glass is also convenient in that it can be poured into the frame of the reinforcement and thus can be further strengthened. As reinforcing elements, metal wire, polysilicate, polymer, polycarbon compounds, which can have a fairly small thickness, can be used. The thickness of such reinforcing materials can be equal to the thickness of several atomic layers, such as graphene.

In [1 – 5], a new approach to solving the problems of impact and nonstationary interaction in the elastoplastic mathematical formulation was developed. In this papers like in nonstationary problems [1 – 5], the action of the striker is replaced by a distributed load in the contact area, which changes according to a linear law. The contact area remains constant. The developed elastoplastic formulation makes it possible to solve impact problems when the dynamic change in the boundary of the contact

area is considered and based on this the movement of the striker as a solid body with a change in the penetration speed is taken into account. Also, such an elastoplastic formulation makes it possible to consider the hardening of the material in the process of nonstationary and impact interaction.

The solution of problems for composite cylindrical shells [6], elastic half-space [7], elastic layer [8], elastic rod [9, 10] were developed using method of the influence functions [11].

In contrast from the work [12], in this paper, we investigate the impact process of hard body with plane area of its surface on the top of the composite beam which consists first thin metal layer and second main glass layer. The fields of plastic deformations and, stresses were determined relative to the size of the area of initial contact.

PROBLEM FORMULATION

Deformations and their increments [13, 14], Odquist parameter, effective and principal stresses are obtained from the numerical solution of the dynamic elastic-plastic interaction problem of infinite composite beam $\{-L/2 \leq x \leq L/2; 0 \leq y \leq B; -\infty \leq z \leq \infty\}$ in the plane of its cross section in the form of rectangle. It is assumed that the stress-strain state in each cross section of the cylinder is the same, close to the plane deformation, and therefore it is necessary to solve the equation for only one section in the form of a rectangle $\Sigma = L \times B$ with two layers: first steel layer $\{-L/2 \leq x \leq L/2; -\infty \leq z \leq \infty; B-h \leq y \leq B\}$ and second glass layer $\{-L/2 \leq x \leq L/2; 0 \leq y \leq B-h; -\infty \leq z \leq \infty\}$ contacts absolute hard half-space $\{y \leq 0\}$. We assume that the contact between the lower surface of the first metal layer and the upper surface of the second glass layer is ideally rigid.

From above on a body the absolutely rigid drummer contacting along a segment $\{|x| \leq A; y = B\}$. Its action is replaced by an even distributed stress $-P$ in the contact region, which changes over time as a linear function $P = p_{01} + p_{02}t$. Given the symmetry of the deformation process relative to the line $x = 0$,

only the right part of the cross section is considered below (Fig. 1). The calculations use known methods for studying the quasi-static elastic-plastic [14, 15 – 17] model, considering the non-stationarity of the load and using numerical integration implemented in the calculation of the dynamic elastic model [1 – 5].

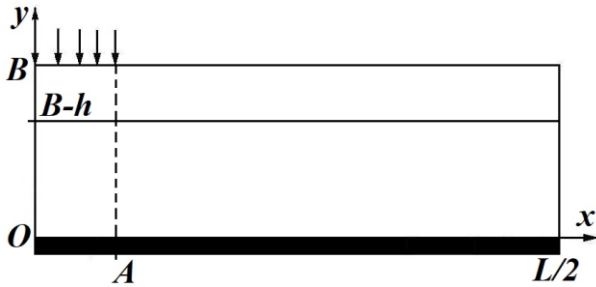


Fig. 1. Geometric scheme of the problem

The equations of the plane dynamic theory are considered, for which the components of the displacement vector $\mathbf{u} = (u_x, u_y)$ are related to the components of the strain tensor by Cauchy relations:

$$\varepsilon_{xx} = \frac{\partial u_x}{\partial x}, \quad \varepsilon_{yy} = \frac{\partial u_y}{\partial y}, \quad \varepsilon_{xy} = \frac{1}{2} \left(\frac{\partial u_x}{\partial y} + \frac{\partial u_y}{\partial x} \right).$$

The equations of motion of the medium have the form:

$$\begin{aligned} \frac{\partial \sigma_{xx}}{\partial x} + \frac{\partial \sigma_{xy}}{\partial y} &= \rho \frac{\partial^2 u_x}{\partial t^2}, \\ \frac{\partial \sigma_{xy}}{\partial x} + \frac{\partial \sigma_{yy}}{\partial y} &= \rho \frac{\partial^2 u_y}{\partial t^2}, \end{aligned} \quad (1)$$

where ρ – material density.

The boundary and initial conditions of the problem have the form:

$$\begin{aligned} x=0, 0 < y < B: u_x &= 0, \sigma_{xy} = 0, \\ x=L/2, 0 < y < B: \sigma_{xx} &= 0, \sigma_{xy} = 0, \\ y=0, 0 < x < L/2: u_y &= 0, \sigma_{xy} = 0, \\ y=B, 0 < x < A: \sigma_{yy} &= -P, \sigma_{xy} = 0, \\ y=B, A < x < L/2: \sigma_{yy} &= 0, \sigma_{xy} = 0. \end{aligned} \quad (2)$$

$$\begin{aligned} u_x|_{t=0} &= 0, u_y|_{t=0} = 0, u_z|_{t=0} = 0, \\ \dot{u}_x|_{t=0} &= 0, \dot{u}_y|_{t=0} = 0, \dot{u}_z|_{t=0} = 0. \end{aligned} \quad (3)$$

The determinant relations of the mechanical

model are based on the theory of non-isothermal plastic flow of the medium with hardening under the condition of Huber-Mises fluidity. The effects of creep and thermal expansion are neglected. Then, considering the components of the strain tensor by the sum of its elastic and plastic components [18, 19], we obtain expression for them:

$$\begin{aligned} \varepsilon_{ij} &= \varepsilon_{ij}^e + \varepsilon_{ij}^p, \quad d\varepsilon_{ij}^p = s_{ij} d\lambda, \\ \varepsilon_{ij}^e &= \frac{1}{2G} s_{ij} + K\sigma + \phi. \end{aligned} \quad (4)$$

here $s_{ij} = \sigma_{ij} - \delta_{ij}\sigma$ – stress tensor deviator; δ_{ij} – Kronecker symbol; E – modulus of elasticity (Young's modulus); G – shear modulus; $K_1 = (1 - 2\nu)/(3E)$, $K = 3K_1$ – volumetric compression modulus, which binds in the ratio $\varepsilon = K\sigma + \phi$ volumetric expansion 3ε (thermal expansion $\phi \equiv 0$); $\sigma = (\sigma_{xx} + \sigma_{yy} + \sigma_{zz})/3$ – mean stress; $d\lambda$ – some scalar function [15], which is determined by the shape of the load surface and we assume that this scalar function is quadratic function of the stress deviator s_{ij} [18, 19].

$$d\lambda = \begin{cases} 0 & (f \equiv \sigma_i^2 - \sigma_S^2(T) < 0) \\ \frac{3d\varepsilon_i^p}{2\sigma_i} & (f = 0, df = 0) \\ (f > 0 - \text{inadmissible}) \end{cases}, \quad (5)$$

$$\begin{aligned} d\varepsilon_i^p &= \frac{\sqrt{2}}{3} \left(\left(d\varepsilon_{xx}^p - d\varepsilon_{yy}^p \right)^2 + \left(d\varepsilon_{xx}^p - d\varepsilon_{zz}^p \right)^2 + \right. \\ &\quad \left. + \left(d\varepsilon_{yy}^p - d\varepsilon_{zz}^p \right)^2 + 6 \left(d\varepsilon_{xy}^p \right)^2 \right)^{1/2}, \\ \sigma_i &= \frac{1}{\sqrt{2}} \left(\left(\sigma_{xx} - \sigma_{yy} \right)^2 + \left(\sigma_{xx} - \sigma_{zz} \right)^2 + \right. \\ &\quad \left. + \left(\sigma_{yy} - \sigma_{zz} \right)^2 + 6\sigma_{xy}^2 \right)^{1/2}. \end{aligned}$$

The material is strengthened with a hardening factor η^* [1, 2, 26 – 28]:

$$\sigma_S(T) = \sigma_{02}(T_0) \left(1 + \frac{\kappa(T)}{\varepsilon_0} \right)^{\eta^*}, \quad (6)$$

$$\varepsilon_0 = \frac{\sigma_{02}(T_0)}{E},$$

where T – temperature; κ – Odquist parameter, $T_0 = 20^\circ C$, η^* – hardening coefficient; $\sigma_S(T)$ – yield strength after hardening of the material at temperature T .

Rewrite (4) in expanded form:

$$d\varepsilon_{xx} = d \left(\frac{\sigma_{xx} - \sigma}{2G} + K\sigma \right) + (\sigma_{xx} - \sigma)d\lambda,$$

$$d\varepsilon_{yy} = d \left(\frac{\sigma_{yy} - \sigma}{2G} + K\sigma \right) + (\sigma_{yy} - \sigma)d\lambda, \quad (7)$$

$$d\varepsilon_{zz} = d \left(\frac{\sigma_{zz} - \sigma}{2G} + K\sigma \right) + (\sigma_{zz} - \sigma)d\lambda,$$

$$d\varepsilon_{xy} = d \left(\frac{\sigma_{xy}}{2G} \right) + \sigma_{xy}d\lambda,$$

In contrast to the traditional plane deformation, when $\Delta\varepsilon_{zz}(x, y) = \text{const}$, for a refined description of the deformation of the specimen, taking into account the possible increase in longitudinal elongation $\Delta\varepsilon_{zz}$, we present in its form [12, 13, 19]:

$$\Delta\varepsilon_{zz}(x, y) = \Delta\varepsilon_{zz}^0 + \Delta\chi_{xx} + \Delta\chi_{yy}, \quad (8)$$

where unknown $\Delta\chi_x$ and $\Delta\chi_y$ describe the bending of the prismatic body (which simulates the plane strain state in the solid mechanics) in the Ozx and Ozy planes, respectively, and $\Delta\varepsilon_{zz}^0$ – the increments according to the detected deformation bending along the fibers $x = y = 0$.

SOLUTION ALGORITHM

Let the nonstationary interaction [1 – 3, 13, 14] occur in a time interval $t \in [0, t_*]$. Then for

every moment of time t :

$$\varepsilon_{xx}^e = \frac{\sigma_{xx} - \sigma}{2G} + K\sigma, \quad \varepsilon_{yy}^e = \frac{\sigma_{yy} - \sigma}{2G} + K\sigma,$$

$$\varepsilon_{zz}^e = \frac{\sigma_{zz} - \sigma}{2G} + K\sigma, \quad \varepsilon_{xy}^e = \frac{\sigma_{xy}}{2G},$$

$$\frac{d\varepsilon_{xx}^p}{dt} = (\sigma_{xx} - \sigma) \frac{d\lambda}{dt}, \quad \frac{d\varepsilon_{xy}^p}{dt} = \sigma_{xy} \frac{d\lambda}{dt}, \quad (9)$$

$$\frac{d\varepsilon_{yy}^p}{dt} = (\sigma_{yy} - \sigma) \frac{d\lambda}{dt},$$

$$\frac{d\varepsilon_{zz}^p}{dt} = (\sigma_{zz} - \sigma) \frac{d\lambda}{dt}.$$

For numerical integration over time, Gregory's quadrature formula [20] of order $m_1 = 3$ with coefficients D_n was used. After discretisation in time with nodes $t_k = k\Delta t \in [0, t_*]$ ($k = 0, K$) for each value k we write down the corresponding node values of deformation increments:

$$\Delta\varepsilon_{xx,k} = B_1\sigma_{xx,k} + B_2\sigma_{yy,k} - \beta_{xx},$$

$$\Delta\varepsilon_{yy,k} = B_2\sigma_{xx,k} + B_1\sigma_{yy,k} - \beta_{yy}, \quad (10)$$

$$\Delta\varepsilon_{zz,k} = \alpha_1\sigma_{zz,k} + \alpha_2(\sigma_{xx,k} - \sigma_{yy,k}) - b_{zz},$$

$$\Delta\varepsilon_{xy,k} = B_3\sigma_{xy,k} - b_{xy},$$

$$B_1 = \frac{\alpha_1^2 - \alpha_2^2}{\alpha_1}, \quad \alpha_1 = \frac{1}{3} \left(K + \frac{1}{G} + 2D_0\Delta\lambda_k \right),$$

$$B_2 = \frac{\alpha_2(\alpha_1 - \alpha_2)}{\alpha_1}, \quad B_3 = \frac{1}{2G} + D_0\Delta\lambda_k,$$

$$\alpha_2 = \frac{1}{3} \left(K - \frac{1}{2G} - D_0\Delta\lambda_k \right),$$

$$\beta_{xx} = b_{xx} - \alpha_2(b_{zz} + \Delta\varepsilon_{zz}) / \alpha_1,$$

$$\beta_{yy} = b_{yy} - \alpha_2(b_{zz} + \Delta\varepsilon_{zz}) / \alpha_1,$$

$$\beta_{zz} = -(b_{zz} + \Delta\varepsilon_{zz}) / \alpha_1,$$

$$b_{ij} = \frac{1}{2G} \sigma_{ij,k-1} + \delta_{ij} \left(K - \frac{1}{2G} \right) \sigma_{k-1} -$$

$$- \sum_{n=1}^{m_1} D_n \left(\sigma_{ij,k-n} - \delta_{ij} \sigma_{k-n} \right) \Delta\lambda_{k-n} \quad (i, j = x, y, z).$$

The solution of the system (10) gives expressions for the components of the stress tensor at each step:

$$\begin{aligned}
 \sigma_{xx,k} &= A_1 \Delta \varepsilon_{xx,k} + A_2 \Delta \varepsilon_{yy,k} + Y_{xx}, \\
 \sigma_{yy,k} &= A_2 \Delta \varepsilon_{xx,k} + A_1 \Delta \varepsilon_{yy,k} + Y_{yy}, \\
 \sigma_{zz,k} &= -\alpha_2 (\sigma_{xx,k} + \sigma_{yy,k}) / \alpha_1 - \beta_{zz}, \\
 \sigma_{xy,k} &= A_3 \Delta \varepsilon_{xy,k} + Y_{xy}, \\
 Y_{xx} &= A_1 \beta_{xx} + A_2 \beta_{yy}, \\
 Y_{yy} &= A_2 \beta_{xx} + A_1 \beta_{yy}, \\
 Y_{xy} &= A_3 b_{xy}, \quad A_3 = 1/B_3, \\
 A_1 &= B_1 / (B_1^2 - B_2^2), \\
 A_2 &= -B_2 / (B_1^2 - B_2^2).
 \end{aligned} \tag{11}$$

Function $\psi = 1/(2G) + \Delta\lambda$, which is characterizing the yield condition, taking into account (8), (9), (11) is:

$$\psi = \begin{cases} \frac{1}{2G} & (f < 0) \\ \frac{1}{2G} + \frac{3\Delta\varepsilon_i^p}{2\sigma_i} & (f = 0, df = 0), \\ (f > 0 - \text{inadmissible}) \end{cases} \tag{12}$$

$$\begin{aligned}
 \Delta\varepsilon_i^p &= \frac{\sqrt{2}}{3} \left((\Delta\varepsilon_{xx}^p - \Delta\varepsilon_{yy}^p)^2 + (\Delta\varepsilon_{xx}^p - \Delta\varepsilon_{zz}^p)^2 + \right. \\
 &\left. + (\Delta\varepsilon_{yy}^p - \Delta\varepsilon_{zz}^p)^2 + 6(\Delta\varepsilon_{xy}^p)^2 \right)^{1/2}, \\
 \Delta\varepsilon_{xx}^p &= \Delta\varepsilon_{xx} - \Delta\varepsilon_{xx}^e, \quad \Delta\varepsilon_{yy}^p = \Delta\varepsilon_{yy} - \Delta\varepsilon_{yy}^e, \\
 \Delta\varepsilon_{xy}^p &= \Delta\varepsilon_{xy} - \Delta\varepsilon_{xy}^e, \quad \Delta\varepsilon_{zz}^p = \Delta\varepsilon_{zz} - \Delta\varepsilon_{zz}^e, \\
 \Delta\varepsilon_{xx}^e &= \frac{1}{2G} \sigma_{xx,k} + \left(K - \frac{1}{2G} \right) \sigma_k, \\
 \Delta\varepsilon_{yy}^e &= \frac{1}{2G} \sigma_{yy,k} + \left(K - \frac{1}{2G} \right) \sigma_k, \\
 \Delta\varepsilon_{zz}^e &= \frac{1}{2G} \sigma_{zz,k} + \left(K - \frac{1}{2G} \right) \sigma_k, \\
 \Delta\varepsilon_{xy}^e &= \frac{1}{2G} \sigma_{xy,k}, \quad \sigma_k = \frac{\sigma_{xx,k} + \sigma_{yy,k} + \sigma_{zz,k}}{3}.
 \end{aligned}$$

Considering when calculating the value $\Delta\varepsilon_{zz}^p$, found that its impact is so small that without reducing the accuracy of calculations can be considered $\Delta\varepsilon_{zz}^p = 0$.

To take into account [13, 14] the physical nonlinearity contained in conditions (12), the method of successive approximations is used, which makes it possible to reduce a nonlinear problem to a sequence of linear problems [15 – 17]:

$$\psi^{(n+1)} = \begin{cases} \psi^{(n)} p + \frac{1-p}{2G}, & \text{if } \sigma_{iS} < -Q, \\ \psi^{(n)}, & \text{if } -Q < \sigma_{iS} < Q, \\ \psi^{(n)} \frac{\sigma_i^{(n)}}{\sigma_S(T)}, & \text{if } \sigma_{iS} > Q, \end{cases}$$

$$\sigma_{iS} = \sigma_i^{(n)} - \sigma_S(T), \tag{13}$$

where Q – the value of the largest deviation of the stress intensity $\sigma_i^{(n)}$ in step n from the strengthened yield strength; n – is the approximation number

Unknown [20] $\Delta\chi_x$, $\Delta\chi_y$ and $\Delta\varepsilon_{zz}^0$ in (8) are determined from the conditions of equilibrium of even with respect to x normal stresses σ_{zz} .

$$\iint_{\Sigma} \sigma_{zz}(x, y) \rho dx dy = M_{\rho}, \quad (\rho = 1, x, y), \tag{14}$$

when $M_1 = M_x = M_y = 0$; where M_1 – projection on the axis Oz of the main vector of contact stresses, and M_x, M_y – corresponding projections of the main moment of the forces acting on the resistance (no torsion, as noted). Given the symmetry of the problem and $\sigma_{zz}(x, y) = \sigma_{zz}(-x, y)$ this equation in case of $\rho = x$ is satisfied automatically.

If we substitute (8) and (11) in (14), taking into account the symmetry of the integration domain with respect to x and the even of functions $\sigma_{xx,k}, \sigma_{yy,k}, b_{zz}$, we have $\Delta\chi_x = 0$. A system of linear algebraic equations is obtained

for the calculation of $\Delta\varepsilon_{zz}^0, \Delta\chi_y$:

$$\Delta\varepsilon_{zz}^0 L_{\rho 1} + \Delta\chi_y L_{\rho y} = \bar{M}_\rho, (\rho = 1, y), \quad (15)$$

$$\bar{M}_\rho = \iint_{\Sigma} \frac{\alpha_2 (\sigma_{xx} + \sigma_{yy}) - b_{zz}}{\alpha_1} \rho r dx dy,$$

$$L_{\rho r} = \iint_{\Sigma} \frac{\rho r dx dy}{\alpha_1}, (r, \rho = 1, x, y).$$

The stresses and strains used above were determined for each unit cell from the numerical solution at each point in time $t_k = k\Delta t$.

NUMERICAL SOLUTION

The explicit scheme of the finite difference method was used with a variable partitioning step along the axes Ox (M elements) and Oy (N elements). The step between the split points was the smallest in the area of the layers contact and at the boundaries of the computational domain. Since the interaction process is fleeting, this did not affect the accuracy in the first thin layer, areas near the boundaries, and the adequacy of the contact interaction modelling.

The use of finite differences [21] with variable partition step for wave equations is justified in [22], and the accuracy of calculations with an error of no more than $O((\Delta x)^2 + (\Delta y)^2 + (\Delta t)^2)$ where $\Delta x, \Delta y$ and Δt – increments of variables: spatial x and y and time t . A low rate of change in the size of the steps of the partition mesh was ensured. The time step was constant.

The resolving system of linear algebraic equations with a banded symmetric matrix was solved by the Gauss method according to the Cholesky scheme.

In [23], during experiments, compact samples were destroyed in 21 – 23 ms. The process of destruction of compact specimens from a material of size and with contact loading as in [23] was modelled in a dynamic elastoplastic formulation, considering the unloading of the material and the growth of a crack according to the local criterion of brittle fracture. The samples were destroyed in 23 ms. This confirms the correctness and adequacy of the developed formulation and model.

Figs. 2 – 29 show the results of calculations of two layers specimens with a hardening factor of the material $\eta^* = 0,05$. The first high layer has made from hard steel. The second main low layer has made from quartz glass. Contact between two layers is an ideal. Calculations were made at the following parameter values: temperature $T = 50^\circ\text{C}$; $L = 60$ mm; $B = 10$ mm; $h = 0.3$ mm; $\Delta t = 3.21 \cdot 10^{-8}$ s; $p_{01} = 8$ MPa; $p_{02} = 10$ MPa; $M = 62$; $N = 100$. The smallest splitting step was 0,005 mm, and the largest 2,6 mm ($\Delta x_{\min} = 0,005$ mm; $\Delta y_{\min} = 0,01$ mm (only the first layer); $\Delta x_{\max} = 2,6$ mm; $\Delta y_{\max} = 0,65$ mm).

Fig. 2 shows plots of the Odquist parameter K in the cell of the first layer, which is located in the centre of the specimen at a depth of 0.25 mm. Solid, dotted, and solid with a circle lines correspond to cases where the size of the contact zone was equal $a = 2A = a_1 = 0.3$ mm, $a = a_2 = 0.5$ mm and $a = a_3 = 0.7$ mm, respectively.

Figs. 3 – 11, 12 – 20, 21 – 29 show the fields of the Odquist parameter K , normal stresses σ_{xx} and σ_{yy} at times $t_1 = 2.57 \cdot 10^{-6}$ s, $t_2 = 3.82 \cdot 10^{-6}$ s and $t_3 = 5.13 \cdot 10^{-6}$ s, respectively.

From Figs. 2 – 5, 12 – 14 and 21 – 23 it can be seen that if the smaller the contact zone then the bigger the plastic deformations, however, at the end of the process of non-stationary interaction, they are of the same degree.

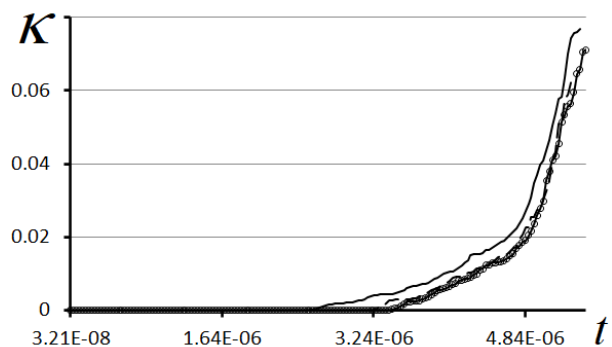


Fig. 2. Odquist parameter K , when $a = a_1, t = t_1$

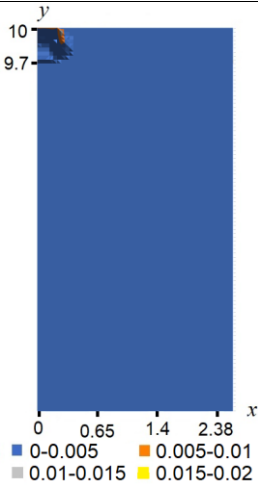


Fig. 3. Odquist parameter K when $a = a_1, t = t_1$



Fig. 4. Odquist parameter K when $a = a_1, t = t_2$



Fig. 5. Odquist parameter K when $a = a_1, t = t_3$

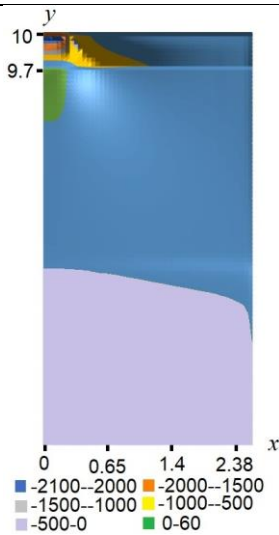


Fig. 6. Stress σ_{xx} when $a = a_1, t = t_1$

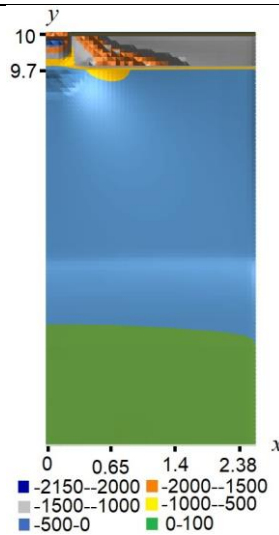


Fig. 7. Stress σ_{xx} when $a = a_1, t = t_2$

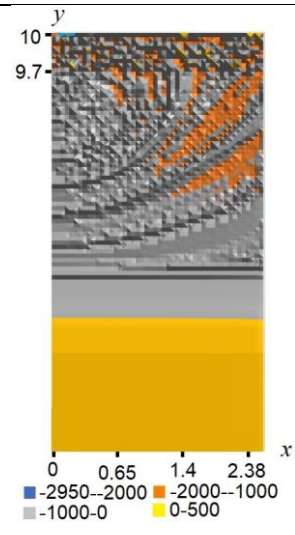


Fig. 8. Stress σ_{xx} when $a = a_1, t = t_3$



Fig. 9. Stress σ_{yy} when $a = a_1, t = t_1$

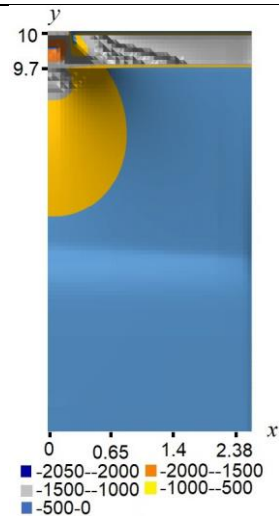


Fig. 10. Stress σ_{yy} $a = a_1, t = t_2$

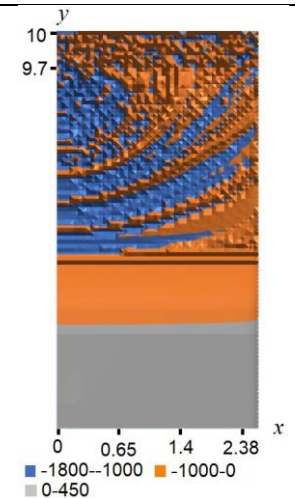


Fig. 11. Stress σ_{yy} $a = a_1, t = t_3$



Fig. 12. Odquist parameter K when $a = a_2, t = t_1$



Fig. 13. Odquist parameter K when $a = a_2, t = t_2$



Fig. 14. Odquist parameter K when $a = a_2, t = t_3$

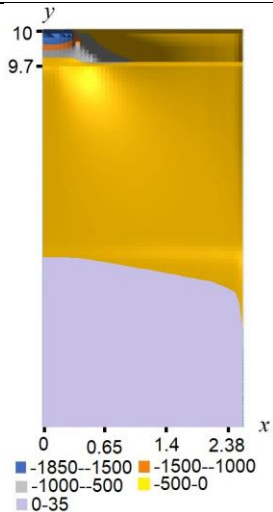


Fig. 15. Stress σ_{xx} when $a = a_2, t = t_1$

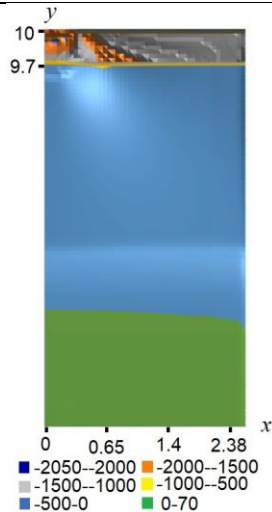


Fig. 16. Stress σ_{xx} when $a = a_2, t = t_2$



Fig. 17. Stress σ_{xx} when $a = a_2, t = t_3$



Fig. 18. Stress σ_{yy} when $a = a_2, t = t_1$

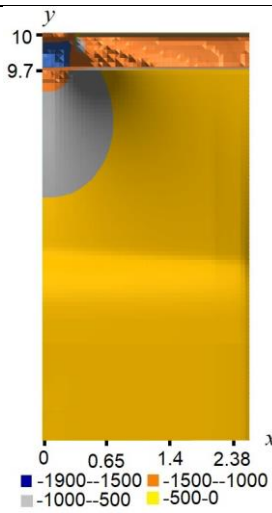


Fig. 19. Stress σ_{yy} when $a = a_2, t = t_2$

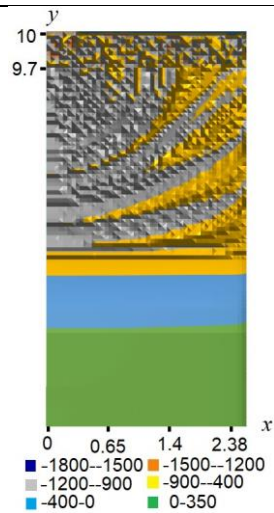


Fig. 20. Stress σ_{yy} when $a = a_2, t = t_3$



Fig. 21. Odquist parameter K when $a = a_3, t = t_1$

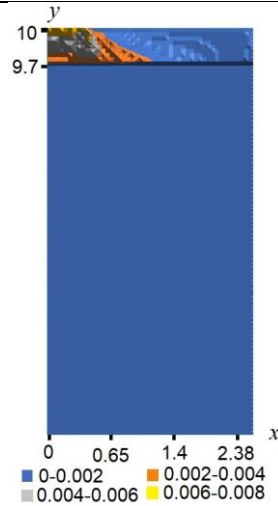


Fig. 22. Odquist parameter K when $a = a_3, t = t_2$



Fig. 23. Odquist parameter K when $a = a_3, t = t_3$

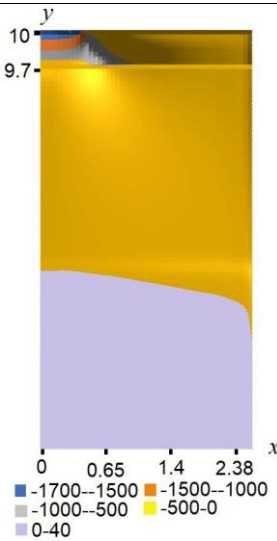


Fig. 24. Stress σ_{xx} when $a = a_3, t = t_1$

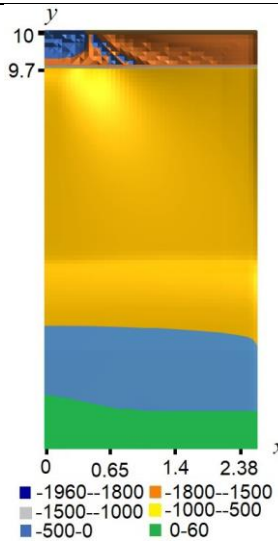


Fig. 25. Stress σ_{xx} when $a = a_3, t = t_2$

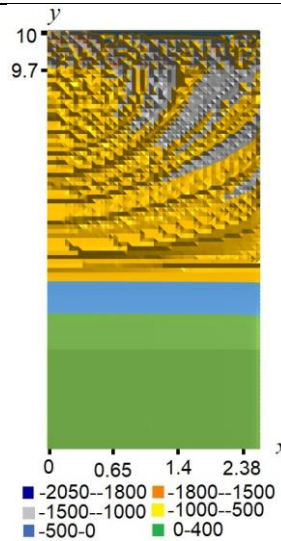


Fig. 26. Stress σ_{xx} when $a = a_3, t = t_3$

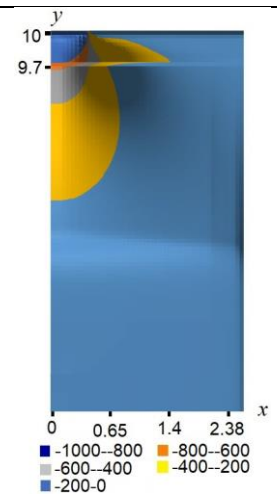


Fig. 27. Stress σ_{yy} when $a = a_3, t = t_1$

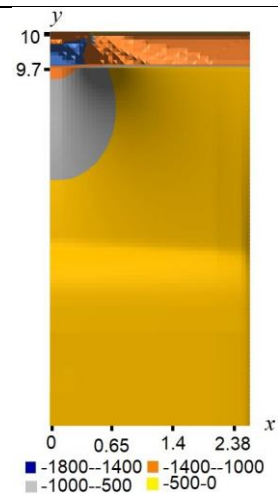


Fig. 28. Stress σ_{yy} when $a = a_3, t = t_2$

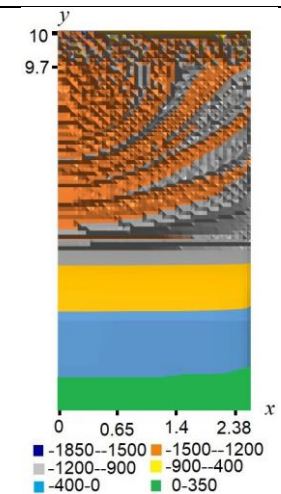


Fig. 29. Stress σ_{yy} when $a = a_3, t = t_3$

Figs. 3 – 29 show that the highest stresses occur in the upper layer of the metal and the process of accumulation of plastic deformations is more intense there. Figs. 6 – 8, 15 – 17, 24 – 26 show areas where the normal stresses σ_{xx} in the lower layer are tensile.

In the case when the contact zone $a = a_1$, at the moment of time $t = t_1$ the area with tensile stresses is located in the middle under the boundary between the layers. This is due to the fact that compressive stresses arise in the upper layer quickly and the contact between the layers is ideally rigid.

Areas where the normal stresses σ_{yy} in the lower layer are tensile are visible from Figs. 11, 20, 29.

At times t_2, t_3 , when the contact zone is a_1 , at times t_1, t_2, t_3 , when the contact zone is equal a_1 and a_2 areas with tensile stresses σ_{xx} in the lower layer are located near its lower boundary.

This is due to the fact that the investigated deformation process has a wave character and the contact of the lower boundary of the lower layer with an absolutely rigid base is ideally rigid.

This also explains that at the moment of time t_3 for all cases of the length of the contact zone, the areas where the normal stresses σ_{yy} are tensile are located near the lower boundary $y = 0$.

CONCLUSIONS

The developed methodology of solving dynamic contact problems in an elastic-plastic dynamic mathematical formulation makes it possible to model the processes of impact, shock and non-stationary contact interaction with the elastic composite base more adequately. In this work, the process of impact on a two-layer base, consisting of an upper thin layer of metal and a lower main layer of glass, is adequately modelled and investigated. The fields of summary plastic deformations and normal stresses arising in the base are calculated depending on the size of the area of an initial contact between the impactor and the upper surface of the base. The area under the stamp in the glass layer under the

metal layer is shown, where there are small tensile normal stresses σ_{xx} , which are most likely due to the propagation of impact waves in the base material. The results obtained make it possible to design new composite reinforced armed materials. Such a two-layer reinforced composite material can be used as a plate of a body armor and a wide range of needs of modern industry.

REFERENCES

1. **Bogdanov V.R., Sulym G.T.** (2013). Plain deformation of elastoplastic material with profile shaped as a compact specimen (dynamic loading). *Mechanics of Solids*, May, 48(4), 329-336; DOI 10.3103/S0025654413030096.
2. **Bogdanov V.R., Sulym G.T.** (2013). A modeling of plastic deformation's growth under impact, based on a numerical solution of the plane stress deformation problem, *Vestnik Moskovskogo Aviatsionnogo Instituta*, Vol.20, Iss.3, 196-201 (in Russian).
3. **Bogdanov V.R., Sulym G.T.** (2012). The plane strain state of the material with stationary crack with taking in account the process of unloading. *Mathematical Methods and Physicomechanical Fields*, Lviv, 55, No.3, 132-138 (in Ukrainian).
4. **Bogdanov V.R., Sulym G.T.** (2010). The crack growing in compact specimen by plastic-elastic model of planar stress state. *Bulletin of University of Kyiv: Series: Physics & Mathematics*, No.4, 58-62 (in Ukrainian).
5. **Bohdanov V.R., Sulym G.T.** (2011). Evaluation of crack resistance based on the numerical modelling of the plane strained state. *Material Science*, 46, No.6, 723-732.
6. **Lokteva N.A., Serduk D.O., Skopintsev P.D., Fedotenkov G.J.** (2020). Non-stationary stress-deformed state of a composite cylindrical shell. *Mechanics of Composite Materials and Structures*, 26(4), 544-559, DOI: 10.33113/mkmmk.ras.2020.26.04.544_559.08 (in Russian).
7. **Igumnov L.A., Okonechnikov A.S., Tarlakovskii D.V., Fedotenkov G.J.** (2013). Plane non-steady-state problem of motion of the surface load on an elastic half-space. *Mathematical Methods and Physicomechanical Fields*, Lviv, 56, No.2, 157-163 (in Russian).
8. **Kuznetsova E.L., Tarlakovsky D.V., Fedotenkov G.J., Medvedsky A.L.** (2013). Influence of non-stationary distributed load on the surface of the elastic layer. *Works MAI*, 71, 1-21 (in Russian).

9. **Fedotenkov G.J., Tarlakovsky D.V., Vahterova Y.A.** (2019). Identification of Non-stationary Load Upon Timoshenko Beam. *Lobachevskii Journal of Mathematics*, 40(4), 439-447.
10. **Vahterova Y.A., Fedotenkov G.J.** (2020). The inverse problem of recovering an unsteady linear load for an elastic rod of finite length. *Journal of Applied Engineering Science*, 18(4), 687-692, DOI:10.5937/jaes0-28073.
11. **Gorshkov A.G., Tarlakovsky D.V.** (1985). Dynamic contact problems with moving boundaries. Nauka, Fizmatlit, 352 (in Russian).
12. **Bogdanov V.R.** (2018). Impact a circular cylinder with a flat on an elastic layer. *Transfer of Innovative Technologies*. Vol.1(2), 68-74, DOI: 10.31493/tit1812.0302.
13. **Bogdanov V.R., Sulym G.T.** (2010). On the solution of the problem of a plane deformed state of a material taking into account elastic-plastic deformations under dynamic loading. *Theoretical and applied mechanics, Donetsk*, No.1(47), 126-133 (in Russian).
14. **Bogdanov V.R.** (2012). The destruction toughness determination on the base of solution of three dimension problem in quasistatic plastic-elastic formulation. *Bulletin of University of Lviv: Series: Physics & Mathematics*, No.76, 65-75 (in Ukrainian).
15. **Mahnenko V.I.** (1976). Computational methods for studying the kinetics of welding stresses and deformations. *Naukova Dumka, Kiev*, 320 (in Russian).
16. **Mahnenko V.I.** (2003). Improving methods for estimating the residual life of welded joints in long-life structures. *Automatic welding, Kiev*, No.10-11, 112-121 (in Russian).
17. **Mahnenko V.I., Pozniakov V.D., Velikoivanenko E.A., Rozynka G.F., Pivtorak N.I.** (2009). Risk of cold cracking when welding structural high-strength steels. *Collection of scientific works Processing of materials in mechanical engineering, National Shipbuilding University*, No.3, 5-12 (in Russian).
18. **Kachanov L.M.** (1969). Fundamentals of the theory of plasticity. Nauka, Moscow, 420 (in Russian).
19. **Collection: Theory of plasticity II** (1948), Moscow, 460. (in Russian)
20. **Boli B., Waner G.** (1964). Theory of thermal stresses. Mir, Moscow, 360 (in Russian).
21. **Hemming R.V.** (1972). Numerical methods. Nauka, Moscow, 399 (in Russian).
22. **Zukina E.L.** (2004). Conservative difference schemes on non-uniform grids for a two-dimensional wave equation. *Work of N.I. Lobachevskii Math. Centre, Kazan*, Vol.26, 151-160 (in Russian).
23. **Weisbrod G., Rittel D.** (2000). A method for dynamic fracture toughness determination using short beams, *International Journal of Fracture*, No.104, 89-103.

Задача о плоском деформированном состоянии двухслойного тела в динамической упругопластической постановке (Часть I)

Владислав Богданов

Аннотация. Проектирование композитных и армированных материалов является требованием современного уровня производства и жизни. С успехом используются многие методы расчетов и проектирования таких материалов. В данной статье для проектирование композитных и армированных материалов используется методика решения динамических контактных задач в упругопластической математической постановке.

Для учета физической нелинейности процесса деформирования используется метод последовательных приближений, позволяющий свести нелинейную задачу к решению последовательности линейных задач. В отличие от традиционной плоской деформации, когда одно нормальное напряжение равняется некоторому постоянному значению, для уточненного описания деформации образца с учетом возможного увеличения продольного удлинения приведем это нормальное напряжение в виде функции, зависящей от параметров, которые описывают изгиб призматического тела, которое находится в состоянии плоской деформации.

Решается задача плоского деформированного состояния композитной балки стеклопакета, которая жестко сцеплена с абсолютно твердым основанием и на которую сверху по центру на небольшой площадке начального контакта действует абсолютно твердый ударник. Стеклопакет состоит из двух слоев: верхний (первый) тонкий из твердой стали и нижний (второй) основной из стекла.

Стекло является очень прочным и очень хрупким материалом одновременно. Хрупкость стекла обуславливается тем, что на поверхности располагается множество микротрещин и при приложении нагрузки к поверхности стекла эти микротрещины начинают расти и приводят к разрушению стеклянных изделий. Если склеить

или обездвижить вершины микротрещин на поверхности, то получим прочный армированный материал, который будет более легким, прочным и не подверженным процессам деградации свойств материала таким, как процессы старения, коррозии и ползучести. Верхний армирующий слой метала можно наносить на поверхность стекла путем напыления так, чтобы атомы

металла стали глубоко проникали, заполняли микротрещины и связывали их вершины. Верхний слой может быть достаточно тонким.

Ключевые слова: Плоская деформация, удар, композитные материалы, армированные материалы, бронированные материалы, упругопластическая, деформация.